ARTICLE
Journal of Cellular Biochemistry 106:93–102 (2009)

Journal of Cellular Biochemistry

Upregulation of Fas and FasL in Taiwan Cobra Phospholipase A_2-Treated Human Neuroblastoma SK-N-SH Cells Through ROS- and Ca^{2+}-Mediated p38 MAPK Activation

Ku-Chung Chen,[1] Pei-Hsiu Kao,[1] Shinne-Ren Lin,[2] and Long-Sen Chang[1]*

[1] *Institute of Biomedical Sciences, National Sun Yat-Sen University-Kaohsiung Medical University Joint Research Center, National Sun Yat-Sen University, Kaohsiung 804, Taiwan*

[2] *Department of Medicinal and Applied Chemistry, Kaohsiung Medical University, Kaohsiung 807, Taiwan*

ABSTRACT

The aim of the present study is to elucidate the signaling pathway involved in death of human neuroblastoma SK-N-SH cells induced by *Naja naja atra* phospholipase A_2 (PLA_2). Upon exposure to PLA_2, p38 MAPK activation, ERK inactivation, ROS generation, increase in intracellular Ca^{2+} concentration, and upregulation of Fas and FasL were found in SK-N-SH cells. SB202190 (p38MAPK inhibitor) suppressed upregulation of Fas and FasL. *N*-Acetylcysteine (ROS scavenger) and BAPTA-AM (Ca^{2+} chelator) abrogated p38 MAPK activation and upregulation of Fas and FasL expression, but restored phosphorylation of ERK. Activated ERK was found to attenuate p38 MAPK-mediated upregulation of Fas and FasL. Deprivation of catalytic activity could not diminish PLA_2-induced cell death and Fas/FasL upregulation. Moreover, the cytotoxicity of arachidonic acid and lysophosphatidylcholine was not related to the expression of Fas and FasL. Taken together, our results indicate that PLA_2-induced cell death is, in part, elicited by upregulation of Fas and FasL, which is regulated by Ca^{2+}- and ROS-evoked p38 MAPK activation, and suggest that non-catalytic PLA_2 plays a role for the signaling pathway. J. Cell. Biochem. 106: 93–102, 2009.

KEY WORDS: PHOSPHOLIPASE A_2; ROS; Ca^{2+}; p38 MAPK ACTIVATION; Fas/FasL UPREGULATION

Neurodegenerative disease, a progressive loss of structure or function and death of neurons, is the subset of neurological disorders that include neuron pathologies, Alzheimer's disease, Parkinson's disease, Huntington's disease and Amyotrophic lateral sclerosis [Camins et al., 2008]. The prevalence of neurodegenerative diseases is increasing rapidly, thus understanding the mechanisms and causes of neurological diseases will be helpful for clinical trial therapy. The enzymes phospholipase A_2 (PLA_2) catalyze specifically the hydrolysis of fatty acid bond at position 2 of 1,2-diacyl-*sn*-phosphoglycerides in the presence of Ca^{2+} [Kini, 1997]. Different forms of PLA_2 are expressed in mammalian nervous tissue, including secretory PLA_2 ($sPLA_2$), cytosolic PLA_2 ($cPLA_2$) and Ca^{2+}-independent PLA_2 ($iPLA_2$) [Sun et al., 2004]. Several lines of evidence show that PLA_2 plays a role in regulating physiological and pathological processes in the central nervous system [Farooqui and Horrocks, 2004; Sun et al., 2004, 2007]. Neuronal cell death due to excessive activation of glutamate receptors is found to be associated with increasing PLA_2 activity and expression [Olney, 2002]. Increased $sPLA_2$ expression in the cerebral cortex after ischemia is suggested to cause neurodegeneration [Sun et al., 2004]. Moreover, $sPLA_2$ is suggested to be an inflammatory factor for Alzheimer's disease [Moses et al., 2007].

Extracellular forms of $sPLA_2$, including those from human and Taipan snake venom, have been reported to cause neuronal excitotoxicity and apoptosis by enhancing the ionotropic glutamate receptors and Ca^{2+} channel activities [Kolko et al., 2002; Rodriguez de Turco et al., 2002; Yagami et al., 2002a,b, 2003a,b; Lin et al., 2004]. Nevertheless, the signaling pathway leading to cell death still remains elusive. In the present study, the cytotoxicity of *Naja naja atra* PLA_2 toward human neuroblastoma SK-N-SH cells was evaluated to explore the signaling pathway of PLA_2-induced neuronal cell death. SK-N-SH cells are chosen due to cellular

Grant sponsor: National Science Council, ROC; Grant number: NSC95-2320-B110-007-MY3; Grant sponsor: National Sun Yat-Sen University–Kaohsiung Medical University Joint Center.

*Correspondence to: Prof. Long-Sen Chang, Institute of Biomedical Sciences, National Sun Yat-Sen University, Kaohsiung 804, Taiwan. E-mail: lschang@mail.nsysu.edu.tw

Received 4 June 2008; Accepted 1 October 2008 • DOI 10.1002/jcb.21979 • 2008 Wiley-Liss, Inc.
Published online 13 November 2008 in Wiley InterScience (www.interscience.wiley.com).

characteristics representative of those in an immature nervous system and exhibit a neuronal phenotype with expression of multiple neurochemical markers [Biedler et al., 1978]. Our data indicate that PLA_2 induces increase in Fas and FasL protein expression on SK-N-SH cells. This effect is initiated by Ca^{2+}- and ROS-mediated p38 MAPK activation. These results suggest that Fas-mediated death pathway is involved in $sPLA_2$-induced death of SK-N-SH cells.

MATERIALS AND METHODS

PLA_2 from the venom of *Naja naja atra* (Taiwan cobra) was isolated as previously described [Chang et al., 1998]. His-47 of PLA_2 was modified with *p*-bromophenacyl bromide (BPB) essentially according to the procedure described in Kao et al. (2008). The enzymatic activity of bromophenacylated PLA_2 (BPB-PLA_2) was measured using the PLA_2 activity kit from Cayman Chemical (Ann Arbor, MI) and was approximate 0.06% of that of PLA_2 (data not shown). Anti-caspase 3 antibodies and anti-caspase 8 antibodies, Z-DEVD-fmk (caspase 3 inhibitor) and Z-IETD-fmk (caspase 8 inhibitor) were obtained from Calbiochem, and anti-β-actin antibodies were the product of Chemicon International Inc. Anti-p38 MAPK, anti-phospho-p38 MAPK, anti-ERK, anti-phospho-ERK, and anti-FasL antibodies were the products of Cell Signaling. Anti-Fas antibodies were obtained from BD Pharmingen. *N*-acetylcysteine (NAC), SB202190, U0126, digitonin, MTT, cyclohexmide, diphenyleneiodonium chloride (DPI), nifedipine, arachidonic acid, and lysophosphatidylcholine (LPC) were purchased from Sigma–Aldrich Inc. BAPTA-AM, Fluo-4 AM and dichlorodihydrofluorescein diacetate (H_2DCFDA) were the products of Molecular Probes. Horseradish peroxidase-conjugated secondary antibodies were obtained from Pierce. Cell culture supplies were purchased from GIBCO/Life Technologies Inc. Unless otherwise specified, all other reagents were of analytical grade.

CELL VIABILITY ASSAY

Human neuroblastoma SK-N-SH cells obtained from ATCC (Rockville, MD) were routinely cultured with Dulbecco's modified Eagle's medium containing 10% fetal calf serum, 2 mM glutamine, and penicillin/streptomycin (100 μg/ml) in an incubator humidified with 95% air and 5% CO_2. Cells were harvested from subconfluent monolayers grown in bottles of 75 cm^2 after their detachment by trypsin (1,500 U/ml) containing 5.3 mM EDTA for 5 min at 37°C. Exponentially growing cells (2×10^4 cells/well) were plated in 96-well plates and treated with PLA_2 or BPB-PLA_2 in serum-free medium after 24 h of growth. Alternatively, SK-N-SH cells were treated with arachidonic acid or LPC for 24 h. For pharmacological experiments, culture cells were pretreated with 100 μM Z-DEVD-fmk, 100 μM Z-IETD-fmk, 10 μM SB202190, 10 μM U0126, 10 μM cycloheximide, 2 mM *N*-acetylcysteine, 10 μM DPI, 30 μM BAPTA-AM or 10 μM nifedipine for 1 h before PLA_2 or BPB-PLA_2 was added. At suitable time intervals, MTT solution was added to each well at a final concentration of 0.5 mg/ml and incubated for 4 h. Formazan crystals resulting from MTT reduction were dissolved by addition of 100 μl DMSO per well. The absorbance was detected at 595 nm using a plate reader.

DETECTION OF Fas AND FasL mRNA EXPRESSION BY REVERSE TRANSCRIPTASE-PCR

Total RNA was isolated from untreated control cells, PLA_2-treated cells or BPB-PLA_2-treated cells using the RNeasy minikit (QIAGEN Inc., Valencia, CA) according to the instructions of the manufacturer. Reverse transcriptase reaction was performed with 2 μg of total RNA using M-MLV reverse transcriptase (Promega) according to the manufacturer's recommendation. A reaction without reverse transcriptase was performed in parallel to ensure the absence of genomic DNA contamination. After initial denaturation at 95°C for 10 min, PCR amplification was performed using GoTaq Flexi DNA polymerase (Promega) followed by 35 cycles at 94°C for 50 s, 58°C for 50 s, and 72°C for 50 s. After a final extension at 72°C for 5 min, PCR products were resolved on 2% agarose gels and visualized by ethidium bromide transillumination under UV light. Primer sequences were as follows: Fas, 5′-CAAGGGATTGGAATTGAGGA-3′ (forward) and 5′-GACAAAGCCACCCCAAGTTA-3′ (reverse); and FasL, 5′-TCTCAGACGTTTTTCGGCTT-3′ (forward) and 5′-AAGAC-AGTCCCCCTTGAGGT-3′ (reverse). The PCR reaction yielded DNA fragments with the size of 449 and 406 bp for Fas and FasL, respectively. Each reverse-transcribed mRNA product was internally controlled by glyceraldehyde-3-phosphate dehydrogenase (GADPH) PCR using primers 5′-GAGTCAACGGATTTGGTCGT-3′ (forward) and 5′-TGTGGTCATGAGTCCTTCCA-3′ (reverse), yielding a 512 bp PCR product. The FasL and Fas reverse transcriptase-PCR products were subsequently confirmed by direct sequencing.

MEASUREMENT OF INTRACELLULAR ROS

H_2DCFDA was employed to detect the intracellular generation of ROS. PLA_2-treated cells or BPB-PLA_2-treated cells were collected and incubated with 10 μM H_2DCFDA (dissolved in DMSO) for 20 min prior to harvesting, then washed with PBS. The fluorescence intensity was measured by Beckman Coulter Paradigm™ Detection Platform with excitation at 485 nm and emission at 530 nm. Protein concentration was measured using the Bradford method (BIO-RAD) with bovine serum albumin as a standard. Results were shown as fold-increase in fluorescence intensity per microgram of proteins compared with the control group.

MEASUREMENT OF INTRACELLULAR Ca^{2+}

The level of intracellular Ca^{2+} was quantified by fluorescence with Fluo-4 AM. The cells were treated with PLA_2 or BPB-PLA_2 for the indicated time periods, and the treated cells were washed with ice-cold PBS. The cells resuspended in 1 ml PBS were incubated with 5 μl of 1 mM Fluo-4 AM for 1 h. The fluorescence intensity of intracellular Ca^{2+} concentration was measured by Beckman Coulter Paradigm™ Detection Platform with excitation at 485 nm and emission at 530 nm. Results were shown as fold-increase in fluorescence intensity per microgram of proteins compared with the control group.

DNA TRANSFECTION

The pCMV-MEK1 used in this experiment is a generous gift from Dr. W. C. Hung (National Sun Yat-Sen University, Taiwan). pCMV-MEK1 vector expressed the constitutively active MEK1 under control of the CMV promoter. The plasmid was transfected into SK-N-SH cells using Pipette-type Electroporator (MicroPorator-MP100, Digital Bio Tech. Co., Korea).

WESTERN BLOT ANALYSIS

After specific treatments, cells were incubated in lysis buffer (20 mM Tris–HCl, pH 7.5, 1% Triton X-100, 1 mM EDTA, 150 mM NaCl, 10% glycerol, 1 mM Na_3VO_4, 50 mM NaF, 1 mM PMSF and protease inhibitor mixtures) for 20 min on ice. After insoluble debris was precipitated by centrifugation at 13,000*g* at 4°C for 15 min, the supernatants were collected and assayed for protein concentration using the Bradford method. An equal amount of protein per sample (15 μg) was resolved on SDS–PAGE and transferred onto a PVDF membrane. The transferred membranes were blocked for 1 h in 5% non-fat milk in PBST (PBS containing 0.05% Tween 20) and incubated with appropriate primary antibodies and horseradish peroxidase-conjugated secondary antibodies. The immune complexes were detected by SuperSignal West Pico Chemiluminescent substrate kit (Pierce).

STATISTICAL ANALYSIS

All data are presented as mean ± SD. Significant differences among the groups were determined using the unpaired Student's *t*-test. A value of $P < 0.05$ was taken as an indication of statistical significance. All the figures shown in this article were obtained from at least three independent experiments with similar results.

RESULTS AND DISCUSSION

PLA_2 INDUCES CASPASE-DEPENDENT DEATH IN HUMAN SK-N-SH CELLS

Upon exposure to PLA_2, SK-N-SH cells showed a concentration-dependent decrease in cell viability (Fig. 1A). This was in line with our previous results showing that PLA_2-induced necrotic cell death

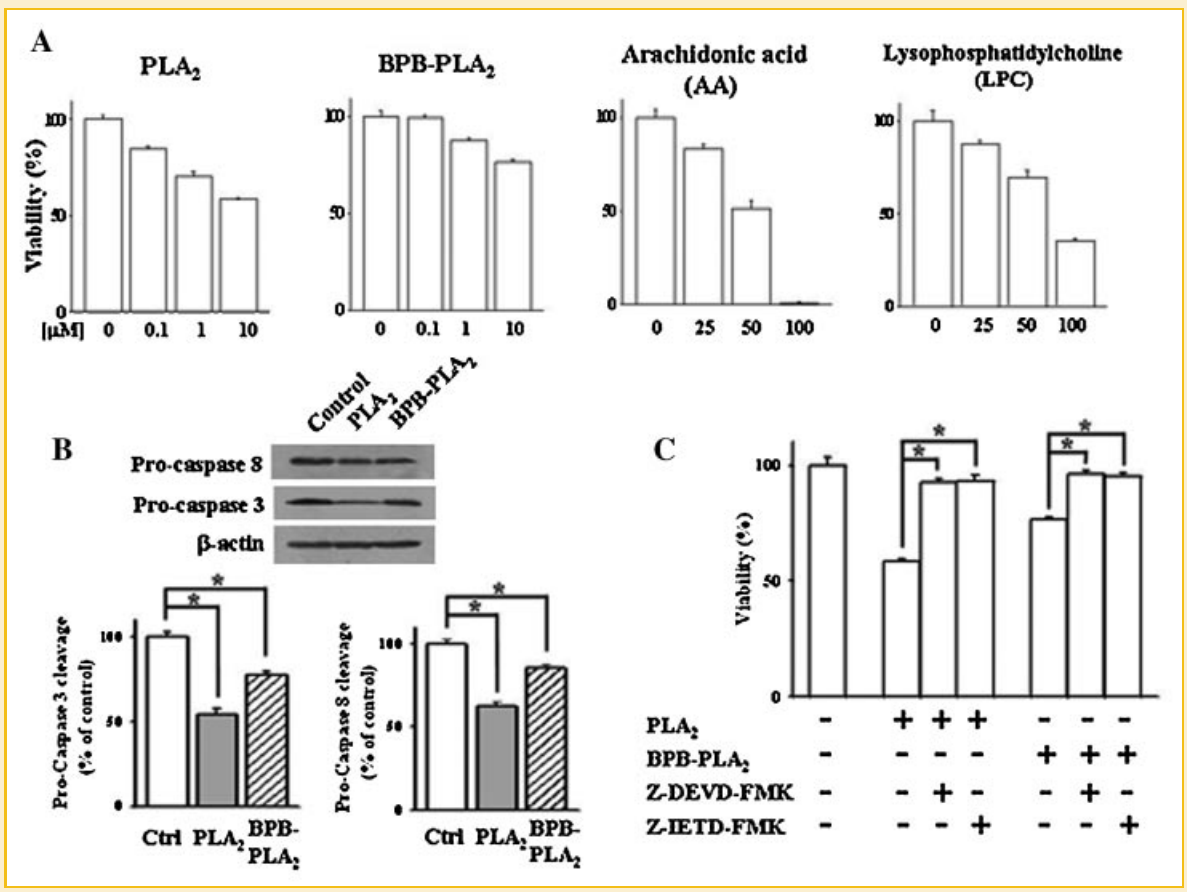

Fig. 1. PLA_2 induced cell death of SK-N-SH cells. A: Concentration-dependent effect of PLA_2, BPB-PLA_2, arachidonic acid (AA), and LPC on cell viability. SK-N-SH cells were incubated with indicated concentration of PLA_2, BPB-PLA_2, arachidonic acid, and LPC for 24 h. Cell viability was measured by MTT assay. The values represent averages of three independent experiments with triplicate measurement (mean ± SD). B: Western blot analyses of degradation of procaspases in PLA_2-treated cells (Top panel). (Bottom panel) Quantification of degradation of procaspases from Western blot analyses. Three independent experimental results were analyzed by densitometry ($^*P < 0.05$). C: Caspase inhibitors rescued viability of PLA_2- and BPB-PLA_2-treated cells. Cells were pretreated with 100 μM Z-DEVD-fmk or Z-IETD-fmk for 1 h and then incubated with 10 μM PLA_2 for 24 h. Cell viability was measured by MTT assay. The values represent averages of three independent experiments with triplicate measurement (mean ± SD; $^*P < 0.05$).

[Chen et al., 2008]. A reduction in approximately 40% cell viability was observed by treating with 10 μM PLA_2 for 24 h. BPB-PLA_2 retained approximate 0.06% enzymatic activity of PLA_2, but the cytotoxicity of BPB-PLA_2 was approximate 50% of that of PLA_2 (Fig. 1A). This suggested that the cytotoxic effect of PLA_2 was not tightly correlated with its catalytic activity. Previous studies suggest that sPLA_2 on neuronal cells may result from its direct effect through hydrolysis of membrane phospholipids and from its indirect effect through liberation of bioactive lipid signaling molecules such as arachidonic acid and lysophospholipid [Farooqui and Horrocks, 2004]. Thus, the cytotoxic effect of arachidonic acid and LPC was examined. Figure 1A showed that arachidonic acid and LPC displayed a concentration-dependent cytotoxicity toward SK-N-SH cells. These reflected that the cytotoxicity of PLA_2 on SK-N-SH cells likely mediated through the hydrolytic products of phospholipids. Immunoblotting analyses using anti-caspase 3 and anti-caspase 8 antibodies revealed a decrease in the level of procaspase 3 and procaspase 8 after PLA_2 or BPB-PLA_2 treatment (Fig. 1C). Figure 1D shows that caspase inhibitors (Z-DEVD-fmk, caspase 3 inhibitor; Z-IETD-fmk, caspase 8 inhibitor) rescued viability of PLA_2- or BPB-PLA_2-treated SK-N-SH cells, suggesting that caspase activation was involved in PLA_2-induced cell death.

PLA_2 TREATMENT INDUCES Fas AND FasL PROTEIN EXPRESSION

Death receptors of the tumor necrosis factor (TNF) family such as Fas and TNFR1 are the best-understood death pathways that recruit FADD and procaspase 8 to the receptor. Recruitment of procaspase 8 through FADD leads to its auto-cleavage and activation, and in turn activates effector caspases such as caspase-3 in causing cell death [Thorburn, 2004]. As shown in Figure 2A, immunoblotting analyses displayed a time-dependent increase in expression of Fas and FasL after treatment with PLA_2 or BPB-PLA_2. Upregulation of Fas and FasL in PLA_2-treated cells was higher than that in BPB-PLA_2-treated cells. Moreover, transcriptional levels of Fas mRNA and FasL mRNA were enhanced by PLA_2 or BPB-PLA_2 treatment as evidenced by RT-PCR assay (Fig. 2B). Figure 2C shows that cycloheximide (inhibitor of protein biosynthesis) inhibited PLA_2- or BPB-PLA_2-induced Fas and FasL protein expression. These data consolidated the importance of transcriptional upregulation of Fas and FasL, as the

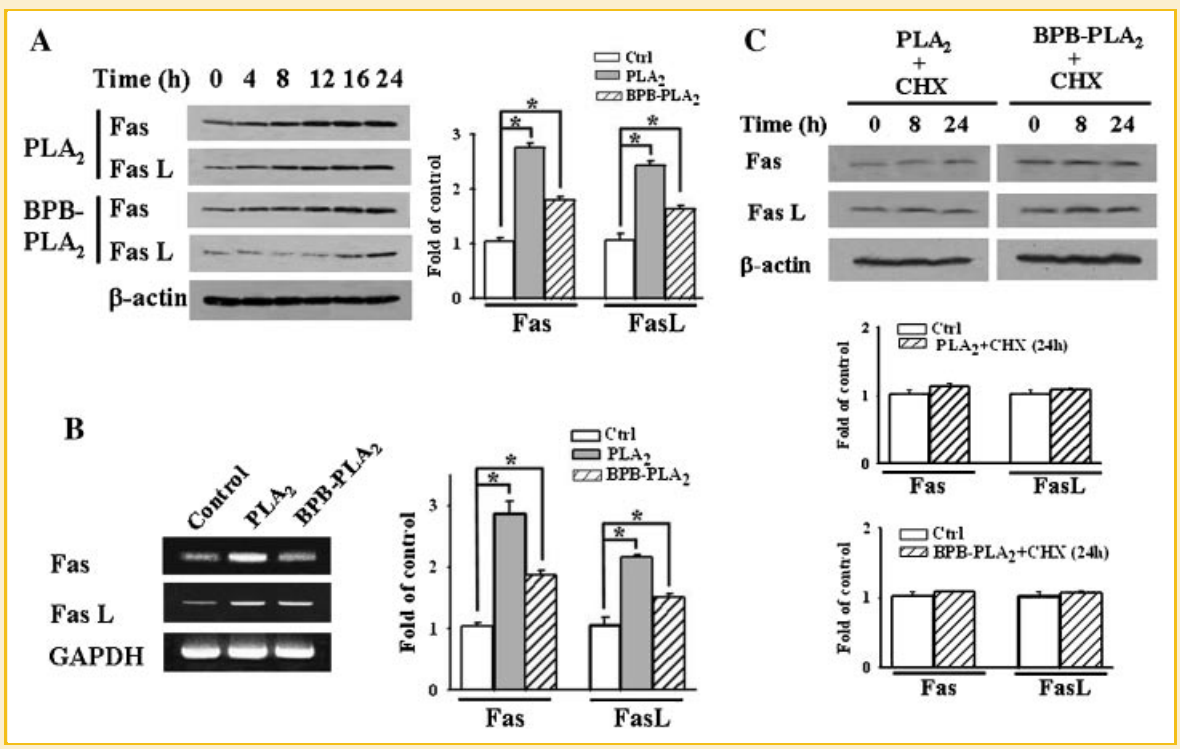

Fig. 2. Upregulation of Fas and FasL in PLA_2- and BPB-PLA_2-treated SK-N-SH cells. A: Western blot analyses of Fas and FasL expression (Left panel). SK-N-SH cells were treated with 10 μM PLA_2 or BPB-PLA_2 for indicated time periods. (Right panel) Quantification of Fas and FasL expression from Western blot analyses. SK-N-SH cells were treated with 10 μM PLA_2 or BPB-PLA_2 for 24 h. Three independent experimental results were analyzed by densitometry ($^*P < 0.05$). B: Detecting the transcription of Fas and FasL mRNA using RT-PCR (Left panel). (Right panel) Quantification of the transcription of Fas and FasL. Three independent experimental results were analyzed by densitometry ($^*P < 0.05$). SK-N-SH cells were treated with 10 μM PLA_2 or BPB-PLA_2 for 24 h. RT-PCR was conducted according to the procedure described in Materials and Methods Section. C: Upregulation of Fas and FasL was suppressed by cycloheximide. (Top panel) Western blot analyses of Fas and FasL. (Bottom panel) Quantification of Fas and FasL expression from Western blot analyses. Three independent experimental results were analyzed by densitometry. SK-N-SH cells were pretreated with 10 μM cycloheximide for 1 h, and then treated with 10 μM PLA_2 or BPB-PLA_2 for 8 h and 24 h. Pretreatment with cycloheximde led to statistically insignificant alteration in the expression of Fas and FasL after PLA_2 and BPB-PLA_2 treatment.

lack of upregulation in the absence of de novo synthesis implies no role for protein stabilization.

PLA_2 INDUCES ACTIVATION OF p38 MAPK

In agreement with our previous studies [Chen et al., 2008], Figure 3A shows that PLA_2 and BPB-PLA_2 increased the level of phospho-p38 MAPK after 24 h treatment. PLA_2 and BPB-PLA_2 induced an increase in phosphorylation of p38 MAPK in a dose-dependent manner, and notable increase in the level of phospho-p38 MAPK was observed when PLA_2 and BPB-PLA_2 was higher than 1 μM. Moreover, upregulation of Fas and FasL was tightly correlated with increase in the level of p38 MAPK. As shown in Figure 3B, pretreatment with SB202190 (p38 MAPK inhibitor) abolished PLA_2- and BPB-PLA_2-induced upregulation of Fas and FasL. Moreover, viability of PLA_2- and BPB-PLA_2-treated cells was also restored by pretreatment with SB202190 (Fig. 3C). These results indicated that p38 MAPK activation was involved in upregulation of Fas and FasL in PLA_2- and BPB-PLA_2-treated SK-N-SH cells.

INACTIVATION OF ERK ENHANCES p38 MAPK-INDUCED UPREGULATION OF Fas AND FasL

As shown in Figure 4A, in sharp contrast to an increase in the level of p38 MAPK, PLA_2 and BPB-PLA_2 induced a time-dependent decrease in the level of phospho-ERK. On the contrary, the level of phospho-JNK was not significantly detected after PLA_2 or BPB-PLA_2 treatment [Chen et al., 2008]. Given that PLA_2 treatment results in a reduction in ERK phosphorylation, it is intriguing to explore whether activated ERK affects p38 MAPK-induced upregulation of Fas and FasL. Expression of constitutively active MEK1 in SK-N-SH cells led to the inability of PLA_2 to inactivate ERK. Compared with control non-transfected cells, PLA_2-induced phosphorylation of p38 MAPK and upregulation of Fas and FasL markedly reduced in pCMV-MEK1-transfected cells. This reflected that activated ERK attenuated p38 MAPK-mediated upregulation of Fas and FasL.

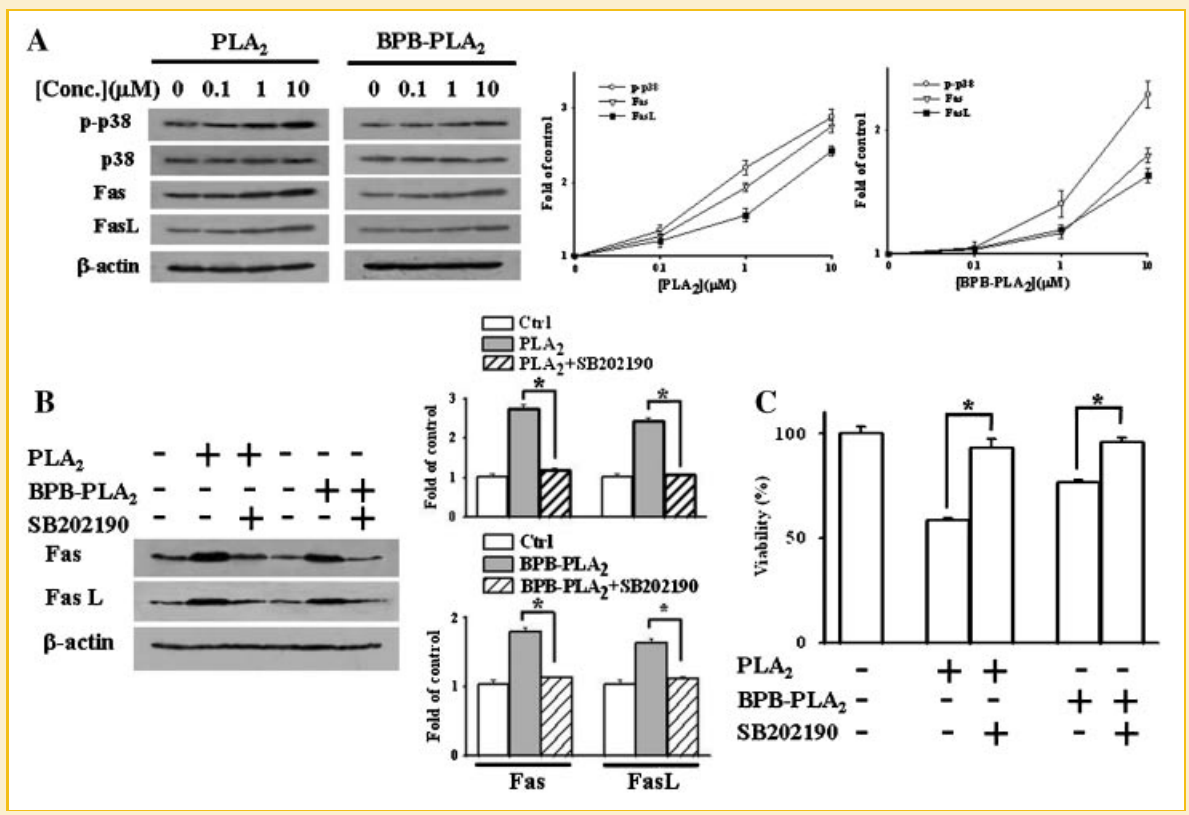

Fig. 3. p38 MAPK activation associated with PLA_2-induced cell death and upregulation of Fas and FasL expression. A: Western blot analyses of phospho-p38 MAPK, Fas and FasL in PLA_2- and BPB-PLA_2-treated cells. (Left panel) SK-N-SH cells were treated with indicated concentrations of PLA_2 or BPB-PLA_2 for 24 h. (Right panel) Quantification of the level of phospho-p38 MAPK, Fas and FasL from Western blot analyses. Three independent experimental results were analyzed by densitometry. B: p38 MAPK inhibitor (SB202190) inhibited PLA_2- and BPB-PLA_2-induced Fas and FasL expression. SK-N-SH cells were pretreated with 10 μM SB202190 for 1 h, and then incubated with 10 μM PLA_2 or BPB-PLA_2 for 24 h. (Left panel) Western blot analyses of Fas and FasL expression. (Right panel) Quantification of Fas and FasL expression. Three independent experimental results were analyzed by densitometry ($^*P < 0.05$). C: Effect of SB202190 on viability of PLA_2- and BPB-PLA_2-treated cells. SK-N-SH cells were pretreated with 10 μM SB202190 (p38 MAPK inhibitor) for 1 h, and then incubated with 10 μM PLA_2 or BPB-PLA_2 for 24 h. Cells viability was analyzed by MTT assay. The values represent averages of three independent experiments with triplicate measurement (mean ± SD; $^*P < 0.05$).

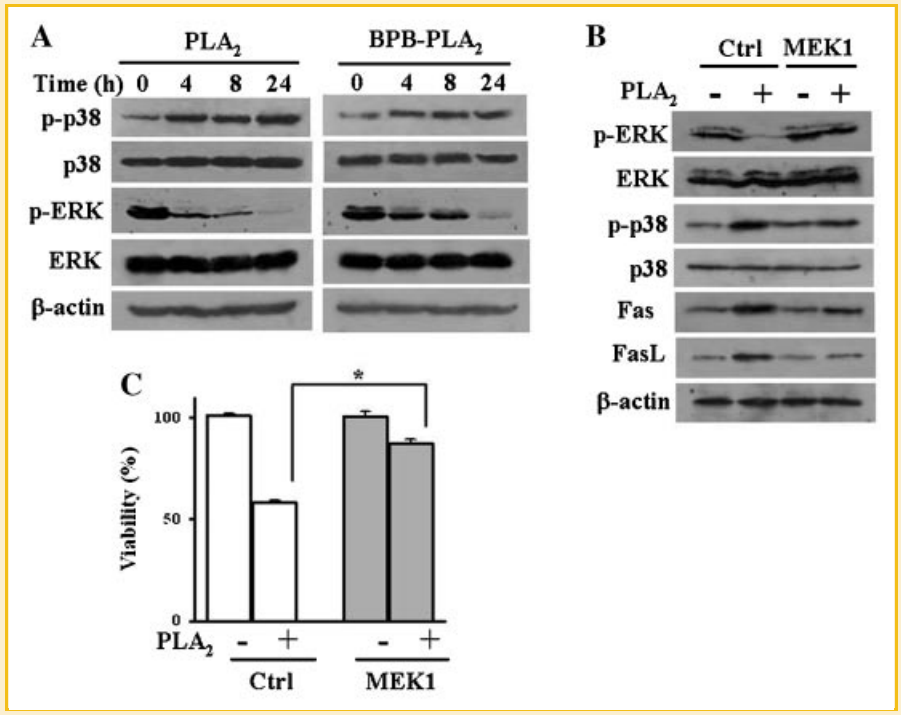

Fig. 4. Activated ERK inhibited p38 MAPK-mediated Fas and FasL upregulation. A: Western blot analyses of phosph-p38 MAPK and phospho-ERK in PLA_2 and BPB-PLA_2-treated cells. SK-N-SH cells were treated with 10 μM PLA_2 or BPB-PLA_2 for indicated time periods. B: Effect of activated ERK on p38 MAPK phosphorylation and the expression of Fas and FasL in PLA_2-treated cells. MEK1 indicated pCMV-MEK1-transfected SK-N-SH cells. Non-transfected and pCMV-MEK1-transfected cells were treated with 10 μM PLA_2 for 24 h. C: Cytotoxicity of PLA_2 on non-transfected and pCMV-MEK1-transfected cells. Non-transfected and pCMV-MEK1-transfected cells were treated with 10 μM PLA_2 for 24 h. Cell viability was measured by MTT assay. The values represent averages of three independent experiments with triplicate measurement (mean ± SD; $^*P < 0.05$).

Moreover, compared with control non-transfected cells, an increase in approximate 25% viability was noted with pCMV-MEK1-transfected cells after PLA_2 treatment.

THE CYTOTOXICITY OF ARACHIDONIC ACID AND LPC IS NOT ASSOCIATED WITH UPREGULATION OF Fas AND FasL

Although arachidonic acid and LPC displayed cytotoxicity, they did not induce an increase in the expression of Fas and FasL (Fig. 5A). Moreover, in sharp contrast to PLA_2, arachidonic acid and LPC did not downregulate phospho-ERK. Nevertheless, p38 MAPK activation was noted with arachidonic acid- and LPC-treated cells. Given that activated ERK inhibited p38 MAPK-mediated Fas and FasL upregulation, it was likely to propose that ERK inactivation may elicit an increase in protein expression of Fas and FasL in arachidonic acid- or LPC-treated cells. Pretreatment with U0126 (ERK inhibitor) led to Fas and FasL upregulation (Fig. 5B) and increasingly reduced the viability of arachidonic acid- and LPC-treated SK-N-SH cells (Fig. 5C). These observations again indicated that activated ERK abrogated p38 MAPK-induced upregulation of Fas and FasL, and suggested that the cytotoxicity of arachidonic acid and LPC was not related to upregulation of Fas and FasL.

p38 MAPK ACTIVATION AND UPREGULATION OF Fas AND FasL ARE EVOKED BY ROS

To assess whether PLA_2 and BPB-PLA_2 treatment induced ROS generation, ROS levels in PLA_2- and BPB-PLA_2-treated cells were measured using H_2DCFDA. As shown in Figure 6A, time-dependent accumulation in ROS levels determined by fluorescent ELISA reader was observed in SK-N-SH cells following PLA_2 or BPB-PLA_2 treatment. Immunoblotting analyses showed that *N*-acetylcysteine (ROS scavenger) abrogated not only p38 MAPK activation but also upregulation of Fas and FasL expression (Fig. 6B). This revealed that ROS was at the upstream of activation of p38 MAPK. Given that oxidative stress arising from activation of NADPH oxidase has been reported to be associated with neurodegenerative disorders [Mathisen et al., 2007; Sun et al., 2007], the effect of DPI (inhibitor of NADPH oxidase) on p38 MAPK activation was assessed. Co-incubation of DPI with PLA_2 or BPB-PLA_2 abolished p38 MAPK activation and upregulation of Fas and FasL (Fig. 6C). It was evident that the action of PLA_2 and BPB-PLA_2 is mediated by ROS generated from NADPH oxidase.

ELEVATION IN INTRACELLULAR Ca^{2+} CONCENTRATION ($[Ca^{2+}]i$) CONTRIBUTES TO p38 MAPK ACTIVATION

Previous studies have reported that $sPLA_2$ enhances Ca^{2+} influx in primary neuronal cultures through stimulation of L-type Ca^{2+} channel [DeCoster et al., 2002; Yagami et al., 2003a,b; Arioka et al., 2005]. As illustrated in Figure 7A,B, it showed that $[Ca^{2+}]i$ was notably increased after treatment with PLA_2 and BPB-PLA_2 for 30 min and then declined to the level indistinguishable from that of untreated control cells. Pretreatment with BAPTA-AM (intracellular Ca^{2+} chelator) or nifedipine (L-type Ca^{2+} channel

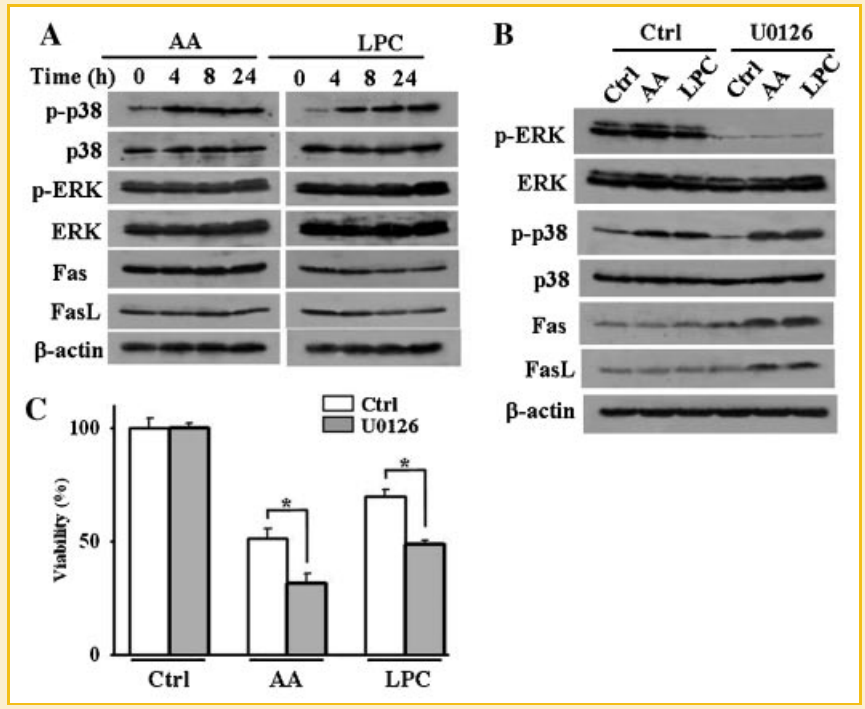

Fig. 5. Effect of arachidonic acid and LPC on the expression of Fas and Fas. A: Western blot analyses of phospho-ERK, phospho-p38 MAPK, Fas and FasL in arachidonic acid- and LPC-treated cells. SK-N-SH cells were treated with 50 μM arachidonic acid or LPC for 24 h. B: Effect of U0126 (ERK inhibitor) on the expression of Fas and FasL in arachidonic acid- or LPC-treated cells. SK-N-SH cells were pretreated with 10 μM U0126 for 1 h, and then incubated with 50 μM arachidonic acid or LPC for 24 h. C: U0126 pretreatment potentiated the cytotoxicity of arachidonic acid and LPC on SK-N-SH cells. SK-N-SH cells were pretreated with 10 μM U0126 for 1 h, and then incubated with 50 μM arachidonic acid or LPC for 24 h. Cell viability was measured by MTT assay. The values represent averages of three independent experiments with triplicate measurement (mean ± SD; $^*P < 0.05$).

blocker) notably attenuated activation of p38 MAPK (inset of Fig. 7A,B). These findings suggest that elevation of intracellular Ca^{2+} should be another upstream regulator in causing p38 MAPK activation. Noticeably, pretreatment with NAC attenuated slightly PLA_2-induced $[Ca^{2+}]i$ increase, while BAPTA-AM notably reduced ROS generation (Fig. 7C,D), indicating that increased $[Ca^{2+}]i$ levels could further induce ROS generation. This is in line with the finding that NADPH oxidase, in response to elevation of cytosolic Ca^{2+}, generated large amount of superoxide [Banfi et al., 2001]. Noticeably, pretreatment with NAC and BAPTA-AM restored ERK phosphorylation in PLA_2-treated cells (Fig. 7E). This suggested that ROS and $[Ca^{2+}]i$ should be upstream events responsible for the inactivation of ERK.

SIGNALING PATHWAY OF PLA_2 IN INDUCING DEATH OF SK-N-SH CELLS

Our data show that the cytotoxicity of BPB-PLA_2 is lower than that of PLA_2, suggesting that the catalytic activity of PLA_2 should contribute to its cytotoxicity. The finding of arachidonic acid and LPC-induced cell death of SK-N-SH cells emphasizes this notion. However, arachidonic acid and LPC are unable to induce the expression of Fas and FasL, suggesting that Fas-mediated death pathway does not strictly depend on catalytic activity of PLA_2. As illustrated in Figure 8, the action of PLA_2 on the upregulation of Fas and FasL is triggered by Ca^{2+}- and ROS-evoked p38 MAPK activation. Moreover, ERK activation plays an inhibitory role in p38 MAPK-induced upregulation of Fas and FasL. Together with the finding that p38 MAPK activation is not completely abolished in pCMV-MEK1-transfected cells after PLA_2 treatment (Fig. 4B), it infers that, in addition to ERK inactivation, ROS and $[Ca^{2+}]i$ play a role in p38 MAPK activation (Fig. 8). Using snake venom $sPLA_2$, Lambeau et al. (1997) identify two specific receptors, N-type and M-type, for $sPLA_2$. Moreover, engagement of M-type receptor in $sPLA_2$-activated MAPK cascade has been reported previously [Hernandez et al., 1998]. Although the cellular target for *N. naja atra* PLA_2 remains to be elucidated, the scenario that non-catalytic PLA_2 elicits ERK/p38 MAPK signaling pathway through the binding with cellular target of PLA_2 can be considered.

Fas/FasL death receptor system is a well-known apoptotic processes that require recruitment of adaptor proteins such as FADD and TRADD to induce activation of caspases [Thorburn, 2004]. However, several studies reveal that Fas-mediated death pathway is involved in necrotic cell death [Siegmund et al., 2007; Villena et al., 2008]. Thus, it is not implausible that PLA_2-induced necrotic death of SK-N-SH cells [Chen et al., 2008] is associated with Fas-mediated death pathway identified in the present study. A number of studies have shown that elevated expression of Fas and FasL is observed in varying neurologic disorders such as infectious, inflammatory, degenerative, infectious, traumatic, neoplastic, developmental, and ischemic disorders [Beer et al., 2000;

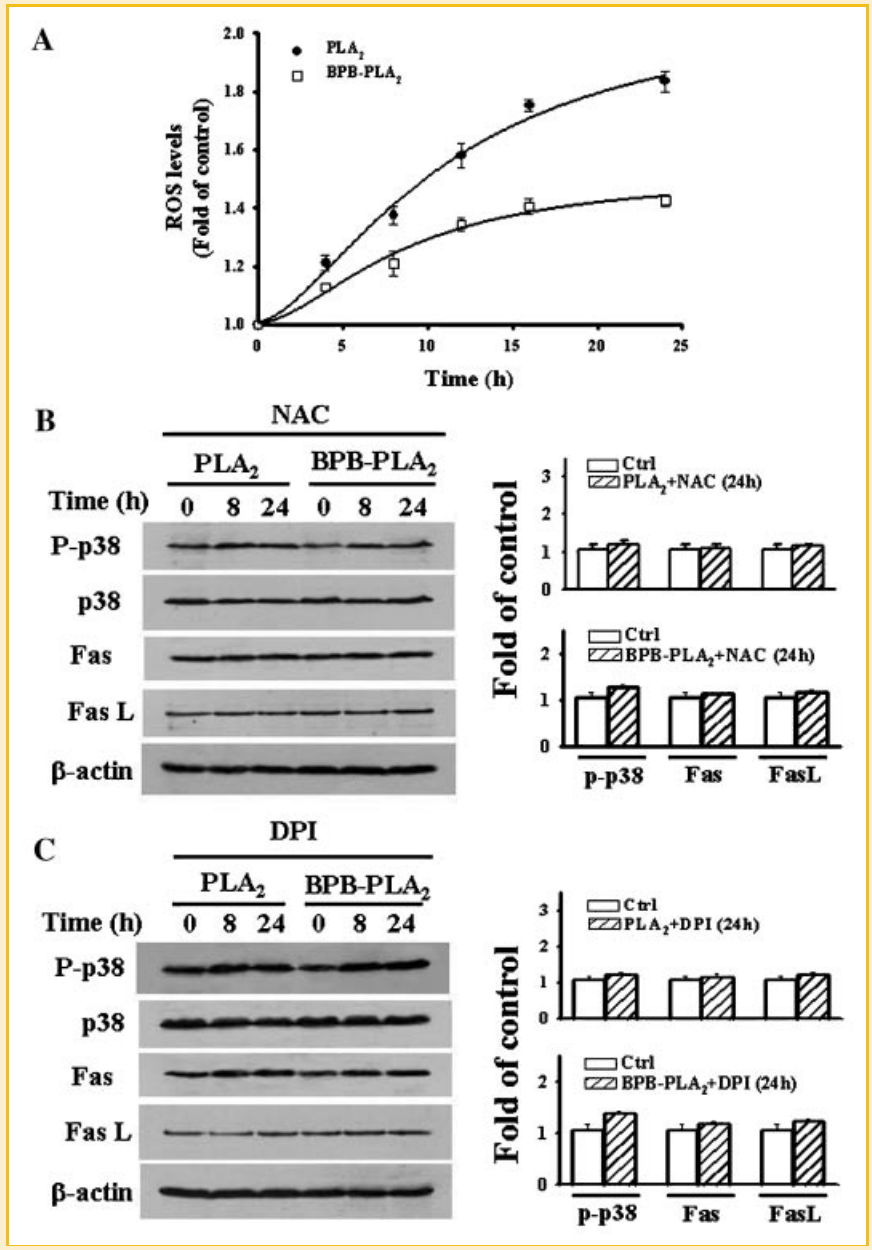

Fig. 6. PLA_2 induced ROS generation in SK-N-SH cells. A: After treatment with 10 μM PLA_2 or BPB-PLA_2 for indicated time periods, ROS generation was quantified by fluorescence plate reader. Results were shown as fold-increase in fluorescence intensity compared with the control group. The data represent the mean ± SD (n = 3). B: Effect of *N*-acetylcysteine (NAC) on PLA_2-induced p38 MAPK activation and upregulation of Fas and FasL. (Left panel) Western blot analyses of phospho-p38 MAPK and the expression of Fas and FasL. (Right panel) Quantification of phospho-p38 MAPK and the expression of Fas and FasL from Western blot analyses. Three independent experimental results were analyzed by densitometry. C: Effect of diphenyleneiodonium chloride (DPI) on PLA_2-induced p38 MAPK activation and upregulation of Fas and FasL. (Left panel) Western blot analyses of phospho-p38 MAPK and the expression of Fas and FasL. (Right panel) Quantification of phospho-p38 MAPK and the expression of Fas and FasL from Western blot analyses. Three independent experimental results were analyzed by densitometry. SK-N-SH cells were pretreated with 2 mM NAC or 10 μM DPI for 1 h, and then incubated with 10 μM PLA_2 or BPB-PLA_2 for 8 h and 24 h. Pretreatment with NAC or DPI led to statistically insignificant alteration in p38 MAPK phosphorylation and the expression of Fas and FasL after PLA_2 and BPB-PLA_2 treatment.

Ferrer et al., 2000, 2001; Li et al., 2000], but little is known about the regulation of Fas and FasL expression in neuron cells during injury. Our data suggest a signaling pathway for *N. naja atra* PLA_2-induced Fas and FasL upregulation, resulting in necrotic death of human neuroblastoma SK-N-SH cells. Growing evidences suggest that $sPLA_2$ plays a critical role in the pathogenesis of CNS injuries and disorders [Sun et al., 2004, 2007; Moses et al., 2007]. Understanding the intracellular signal pathway of $sPLA_2$ in inducing neuronal cell death should be beneficial for elucidating the mechanism of neurodegenerative diseases.

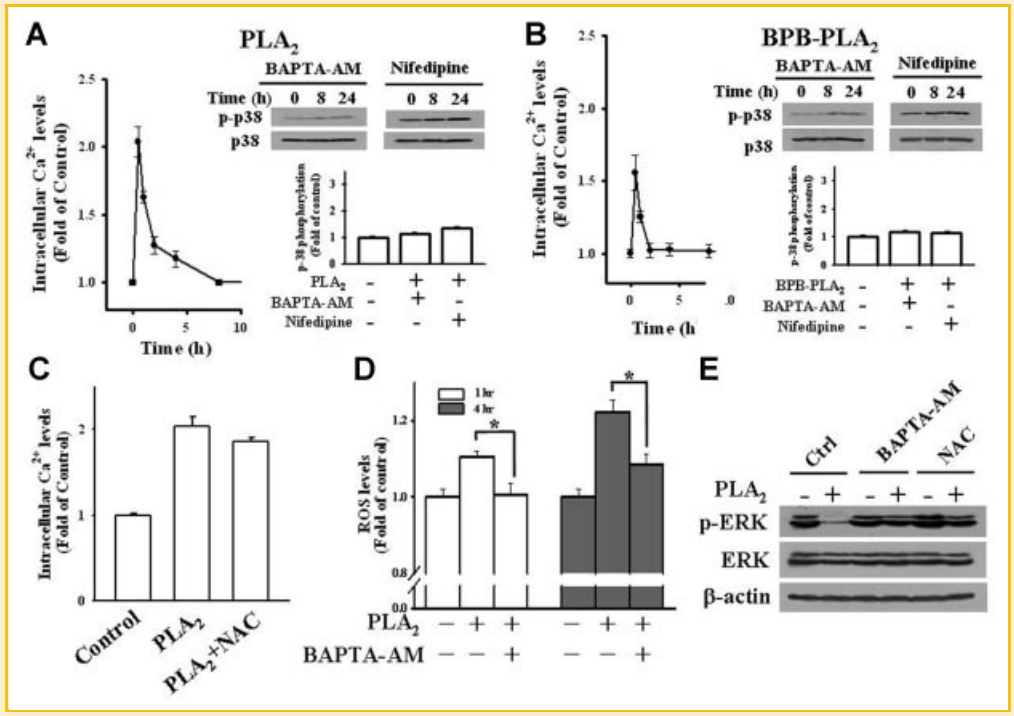

Fig. 7. BAPTA-AM and nifedipine suppressed p38 MAPK activation in PLA_2- and BPB-PLA_2-treated SK-N-SH cells. Elevation of intracellular Ca^{2+} concentration was noted with SK-N-SH cells treated with 10 μM PLA_2 (A) or BPB-PLA_2 (B). Intracellular Ca^{2+} concentration was quantified by fluorescence plate reader after loading the cells with a calcium indicator (Fluo-4 AM). Results were shown as fold-increase in fluorescence intensity compared with the control group. The data represent the mean ± SD (n = 3). Inset: Western blot analyses showed that BAPTA-AM (Ca^{2+} chelator) and nifedipine (L-type Ca^{2+} channel inhibitor) suppressed PLA_2- and BPB-PLA_2-induced p38 MAPK activation (Top panel). Quantification of phospho-p38 MAPK from Western blot analyses (Bottom panel of inset). Three independent experimental results obtained from 24-h PLA_2 or BPB-PLA_2 treatment were analyzed by densitometry. SK-N-SH cells were pretreated with 30 μM BAPTA-AM or 10 μM nifedipine for 1 h, and then incubated with 10 μM PLA_2 or BPB-PLA_2 for 8 h and 24 h. Pretreatment with BAPTA-AM and nifedipine led to statistically insignificant alteration in p38 MAPK phosphorylation after PLA_2 and BPB-PLA_2 treatment. C: Pretreatment with NAC affected PLA_2-induced $[Ca^{2+}]i$ increase marginally. Ca^{2+} levels were measured after treatment with 10 μM PLA_2 for 30 min. D: Pretreatment with BAPTA-AM reduced ROS generation in PLA_2-treated cells. ROS levels were measured after treatment with PLA_2 for indicated time periods. (n = 3, $^*P < 0.05$). E: Effect of BAPTA-AM and NAC on ERK phosphorylation. SK-N-SH cells were pretreated with 30 μM BAPTA-AM or 2 mM NAC for 1 h, and then incubated with 10 μM PLA_2 for 24 h.

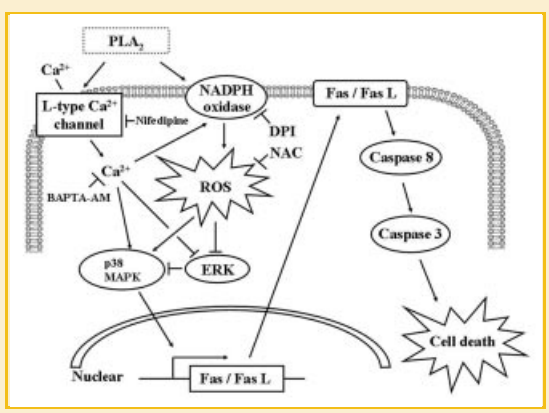

Fig. 8. Signaling pathway of PLA_2 in inducing cell death of SK-N-SH cells. PLA_2 treatment led to increase in $[Ca^{2+}]i$ and ROS levels, which activated p38 MAPK and inactivated ERK. Inactivation of ERK potentiates p38 MAPK phosphorylation, and then activated p38 MAPK upregulated Fas and FasL protein expression. Finally, Fas-mediated death pathway triggered caspase activation and cell death. Our data suggest that elevated $[Ca^{2+}]i$ can further enhance ROS generation. However, the possibility that Ca^{2+} activates p38 MAPK directly is not excluded.

ACKNOWLEDGMENTS

This work was supported by grant NSC95-2320-B110-007-MY3 from the National Science Council, ROC (to L.S. Chang), and grant of National Sun Yat-Sen University–Kaohsiung Medical University Joint Center.

REFERENCES

Arioka M, Cheon SH, Ikeno Y, Nakashima S, Kitamoto K. 2005. A novel neurotrophic role of secretory phospholipase A_2 for cerebellar granule neurons. FEBS Lett 579:2693–2701.

Banfi B, Molnar G, Maturana A, Steger K, Hegedus B, Demaurex N, Krause KH. 2001. A Ca^{2+}-activated NADPH oxidase in testis, spleen and lymph nodes. J Biol Chem 276:37594–37601.

Beer R, Franz G, Schopf M, Reindl M, Zelger B, Schmutzhard E, Poewe W, Kampfl A. 2000. Expression of Fas and Fas ligand after experimental traumatic brain injury in the rat. J Cereb Blood Flow Metab 20:669–677.

Biedler JL, Roffler-Tarlov S, Schachner M, Freedman LS. 1978. Multiple neurotransmitter synthesis by human neuroblastoma cell lines and clones. Cancer Res 33:2643–2652.

Camins A, Pallas M, Silvestre JS. 2008. Apoptotic mechanisms involved in neurodegenerative diseases: Experimental and therapeutic approaches. Methods Find Exp Clin Pharmacol 30:43–65.

Chang LS, Lin SR, Chang CC. 1998. Identification of Arg-30 as the essential residue for the enzymatic activity of Taiwan cobra phospholipase A_2. J Biochem (Tokyo) 124:764–768.

Chen KC, Kao PH, Lin SR, Chang LS. 2008. p38 MAPK activation and mitochondrial depolarization mediate the cytotoxicity of Taiwan cobra phospholipase A_2 on human neuroblastoma SK-N-SH cells. Toxicol Lett 180:53–58.

DeCoster MA, Lambeau G, Lazdunski M, Bazan NG. 2002. Secreted phospholipase A_2 potentiates glutamate-induced calcium increase and cell death in primary neuronal cultures. J Neurosci Res 67:634–645.

Farooqui AA, Horrocks LA. 2004. Brain phospholipases A_2: A perspective on the history. Prostaglandins Leukot Essent Fatty Acids 71:161–169.

Ferrer I, Blanco R, Cutillas B, Ambrosio S. 2000. Fas and Fas-L expression in Huntington's disease and Parkinson's disease. Neuropathol Appl Neurobiol 26:424–433.

Ferrer I, Puig B, Krupinsk J, Carmona M, Blanco R. 2001. Fas and Fas ligand expression in Alzheimer's disease. Acta Neuropathol 102:121–131.

Hernandez M, Burillo SL, Crespo MS, Nieto ML. 1998. Secretory phospholipase A_2 activated the cascade of mitogen-activated protein kinases and cytosolic phospholipase A_2 in the human astrocytoma cell line 1321N1. J Biol Chem 273:606–612.

Kao PS, Chen KC, Lin SR, Chang LS. 2008. The structural and functional contribution of N-terminal region and His-47 on Taiwan cobra phospholipase A_2. J Pept Sci 14:342–348.

Kini RM. 1997. Phospholipase A_2-a complex multifunctional protein puzzle. In: Kini RM, editor. Venom phospholipase A_2 enzymes: Structure, function and mechanism. Chichester: John Wiley & Sons. pp 1–28.

Kolko M, Rodriguez de Turco EB, Diemer NH, Bazan NG. 2002. Secretory phospholipase A_2-mediated neuronal cell death involves glutamate ionotropic receptors. Neuroreport 13:1963–1966.

Lambeau G, Cupillard L, Lazdunski M. 1997. Membrane receptors for venom phospholipases A_2. In: Kini RM, editor. Venom phospholipase A_2 enzymes: Structure, function and mechanism. Chichester: John Wiley & Sons. pp 389–412.

Li GL, Farooque M, Olsson Y. 2000. Changes of Fas and Fas ligand immunoreactivity after compression trauma to rat spinal cord. Acta Neuropathol 100:75–81.

Lin TN, Wang Q, Simonyi A, Chen JJ, Cheung WM, He YY, Xu J, Sun AY, Hsu CY, Sun GY. 2004. Induction of secretory phospholipase A_2 in reactive astrocytes in response to transient focal cerebral ischemia in the rat brain. J Neurochem 90:637–645.

Mathisen GH, Thorkildsen IH, Paulsen RE. 2007. Secretory PLA_2-IIA and ROS generation in peripheral mitochondria are critical for neuronal death. Brain Res 1153:43–51.

Moses GSD, Jensen MD, Lue LF, Walker DG, Sun AY, Simonyi A, Sun GY. 2007. Secretory PLA_2-IIA: A new inflammatory factor for Alzheimer's disease. J Neuroinflammation 3:28.

Olney JW. 2002. New insights and new issues in developmental neurotoxicology. Neurotoxicology 23:659–668.

Rodriguez deTurco EB, Jackson FR, DeCoster MA, Kolko M, Bazan NG, 2002. Glutamate signalling and secretory phospholipase A_2 modulate the release of arachidonic acid from neuronal membranes. J Neurosci Res 68:558–567.

Siegmund D, Klose S, Zhou D, Baumann B, Roder C, Kalthoff H, Wajant H, Trauzold A. 2007. Role of caspases in CD95L- and TRAIL-induced non-apoptotic signalling in pancreatic tumour cells. Cell Signal 19:1172–1184.

Sun GY, Xu J, Jensen MD, Simonyi A. 2004. Phospholipase A_2 in central nervous system: Implications for neurodegenerative diseases. J Lipid Res 45:205–213.

Sun GY, Horrocks LA, Farooqui AA. 2007. The roles of NADPH oxidase and phospholipases A_2 in oxidative and inflammatory responses in neurodegenerative diseases. J Neurochem 103:1–16.

Thorburn A. 2004. Death receptor-induced cell killing. Cell Signal 16:139–144.

Villena J, Henriquez M, Torres V, Moraga F, Díaz-Elizondo J, Arredondo C, Chiong M, Olea-Azar C, Stutzin A, Lavandero S, Quest AFG. 2008. Ceramide-induced formation of ROS and ATP depletion trigger necrosis in lymphoid cells. Free Radic Biol Med 44:1146–1160.

Yagami T, Ueda K, Asakura K, Hayasaki-Kajiwara Y, Nakazato T, Sakaeda T, Hata S, Kuroda K, Takasu N, Hori Y. 2002a. Group IB secretory phospholipase A induces neuronal cell death via apoptosis. J Neurochem 81:449–461.

Yagami T, Ueda K, Asakura K, Hata S, Kuroda T, Sakaeda T, Takasu N, Tanaka K, Gemba T, Hori Y. 2002b. Human group IIA secretory phospholipase A induces neuronal cell death via apoptosis. Mol Pharmacol 61:114–126.

Yagami T, Ueda K, Asakura K, Sakaeda T, Hata S, Kuroda T, Sakaguchi G, Itoh N, Hashimoto Y, Hori Y. 2003a. Porcine pancreatic group IB secretory phospholipase A_2 potentiates Ca^{2+} influx through L-type voltage-sensitive Ca^{2+} channels. Brain Res 960:71–80.

Yagami T, Ueda K, Asakura K, Sakaeda T, Nakazato H, Hata S, Kuroda T, Sakaguchi G, Itoh N, Hashimoto Y, Hori Y. 2003b. Human group IIA secretory phospholipase A potentiates Ca^{2+} influx through L-type voltage-sensitive Ca^{2+} channel. J Neurochem 85:749–758.